ICWE14
June 21-26, 2015 | Porto Alegre - Brazil
14th INTERNATIONAL CONFERENCE ON WIND ENGINEERING

Viscous Treatment of the Snow Phase in Eulerian-Eulerian Simulations of Drifting Snow

Ziad Boutanios[1,2], Hrvoje Jasak[1]
[1]Faculty of Mechanical Engineering and Naval Architecture, University of Zagreb, Croatia
[2]Binkz Inc., Montréal, Canada
email: ziad@binkz.ca, hrvoje.jasak@fsb.hr

ABSTRACT: A novel viscosity model for drifting snow was developed to meet the CFD modeling requirements of drifting snow using a fully two-way coupled Eulerian-Eulerian formulation. This approach allowed explicit resolution of the saltation layer without resorting to empiricism, unlike other Eulerian-Eulerian models. Initial validations were carried out against detailed snow flux, snow transport, airflow, and turbulence measurements in a controlled experimental simulation of a non-equilibrium saltation layer in a wind tunnel using actual snow particles. The two-way coupled approach using the novel viscosity model was found capable to accurately simulate drifting snow in the saltation layer and agreed with the experimental findings in general. Recommendations were made to improve the turbulence modeling, improve the method's accuracy in the suspension layer and to allow simulating a drifting snow phase with a particle size distribution.

KEY WORDS: Drifting Snow, Eulerian, Viscosity, Gamma Distribution, Wind Tunnel, Suspension Layer, Saltation Layer, Snow Flux, K-Epsilon, Particle Collision.

1 INTRODUCTION

Drifting snow results from the aeolian motion of snow particles deposited on the ground. Such motion is possible when the drag force induced by the wind exceeds the opposing actions of inter-particle cohesive bonding, particle weight and surface friction. Particle collisions help sustain drifting even when the particle motion extracts so much momentum from the airflow in the saltation layer that the surface shear stress falls below the aerodynamic entrainment threshold also called the "fluid" threshold. At that point the collision-reduced threshold shear stress is referred to as the "impact" threshold, both definitions first coined by Bagnold [1] in his investigations of desert sand transport by the wind. Bagnold also classified the aeolian motion of particles under three modes, creeping, saltation and suspension. These modes are shown in Figure 1 as they pertain to drifting snow. Of particular interest to this research is the two-way coupled saltation mode.

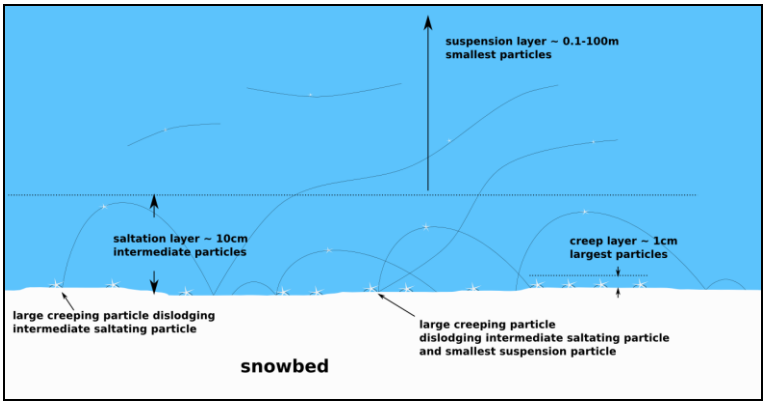

Figure 1. Different modes of drifting snow.

Several aeolian snow transport models are available in the literature. Most are based on Reynolds Averaged Navier-Stokes (RANS) formulations in the Eulerian-Eulerian and Eulerian-Lagrangian frames regarding the air and

snow phases respectively. Both approaches can yield reasonable results for particle-laden flows compared to experiments but the Eulerian-Eulerian approach requires much less computational resources since Lagrangian particle tracking requires a great deal of particles to yield statistically meaningful results [2].

Presently, Eulerian-Eulerian modeling of drifting snow is based on two main approaches, the transport of snowdrift density approach and the Volume of Fluid (VOF) approach. The former approach solves a one-way coupled Partial Differential Equation (PDE) for the drifting snow density in the suspension layer (where the snow phase motion does not affect the airflow, a valid assumption in the suspension layer) in addition to the airflow continuity and momentum equations with a Prandtl mixing layer model [3]. Others use the mixture continuity and momentum equations with a standard K-epsilon turbulence model corrected for turbulence damping by particles [4]. Another application of the snowdrift density approach uses the airflow continuity and momentum equations with a modified Launder-Kato K-epsilon turbulence model [5]. The drifting snow density is transported by the wind velocity, the snowfall velocity is taken constant and the saltation layer, which is not resolved, is represented by a steady-state empirical formulation of the transport rate of drifting snow in the saltation layer for equilibrium conditions over natural flat terrain [6]. However, this empirical representation of the saltation layer has been experimentally shown to overestimate the transport rate of drifting snow in accelerating and decelerating flows [7]. This makes such a representation of the empirical layer at best conservative for flows around bluff bodies where important regions of accelerating and decelerating flows routinely occur. The snowdrift density approach with the Launder-Kato turbulence model has been lately modified to account for snow particle damping of turbulence and with saltation computed with the snowdrift density one-way coupled transport equation, without the empirical saltation flux relationships [8]. These modifications resulted in some improvement but substantial deviations remain from experimental measurements of the snow surface in the lateral vicinity of a cube structure, where accelerating and decelerating effects of bluff body aerodynamics dominate. The computation overestimates the snow accumulation in the stagnation zone ahead of the cube where the flow is reasonably steady-state, and is quite good behind it but one has to wonder whether accumulation behind the cube is due to snowfall or snowdrift.

The VOF approach is a one-way coupling interface tracking method that treats the snow phase as a fluid and relies on the assumption that the fluids are not interpenetrating. Tracking of the interface between the phases is done by solving a continuity equation of one or more of the phases, in addition to the mixture continuity and momentum equations. The phases' relative velocity is based on drift-flux theory which assumes low drift [9], a reasonable assumption for smaller particles only. The VOF approach relies on the same steady-state empirical equilibrium saltation flux treatment as the transport of snowdrift density approach. Different attempts at improving the VOF approach by accounting for particle impingement in saltation as well as modifications of the turbulent wall function roughness parameter based on experiment-specific measurements did not show decisive qualitative improvement compared to experiment especially close to bluff bodies where accelerating and decelerating flows dominate [10]. No decisive improvement was seen either by using mesh adaptation based on the balance of the convected horizontal snow flux using flow divergence at the ground [11]. Yet another application of the VOF approach uses two different snow phase continuity equations, one with mass diffusion and a suspension particle settling velocity in the suspension layer and another without mass diffusion and a saltation particle settling velocity in the saltation layer [12]. The implementation is ripe with ad-hoc empirical coefficients and parameters and does not improve on the previously mentioned limitations.

An exception to both approaches above is Gauer's approach [13] which resolves the saltation layer but still uses considerable parameterization and self-similarity assumptions between the airflow profile and the snow concentration profile in the saltation layer that do not necessarily hold true in the vicinity of bluff bodies. In particular the air velocity and snow concentration profiles in the saltation layer are assumed and related to the air velocity on top of the saltation layer obtained from the suspension layer computation. Gauer's simulations manage to capture the general trends in comparisons of experimental snowdrift rates, wind field velocity and new-snow depth for an Alpine crest. In all fairness much of the discrepancies are due to poor terrain accuracy and large uncertainty in choosing the correct numerical boundary conditions but the results are inconclusive nonetheless.

In contrast to the approaches above a full two-way coupled computation with no empiricism [14], where a Navier-Stokes system is solved for each phase and the two systems are coupled with drag forces, managed to reproduce the experimental snowdrift profile around a tilted cube model much better than the VOF approach [15]. The simulation was done with the twoPhaseEulerFoam solver, which is part of the OpenFOAM® CFD toolkit. The conditional ensemble-averaged equations of conservation of mass and linear momentum used to represent the interpenetrating phases are respectively,

ICWE14 June 21-26, 2015 | Porto Alegre - Brazil 14th INTERNATIONAL CONFERENCE ON WIND ENGINEERING

$$\frac{\partial \alpha_k \rho_k}{\partial t} + \nabla \cdot \alpha_k \rho_k \mathbf{u}_k = 0 \tag{1}$$

$$\frac{\partial \alpha_k \rho_k \mathbf{u}_k}{\partial t} + \nabla \cdot \alpha_k \rho_k \mathbf{u}_k \mathbf{u}_k = -\alpha_k \nabla p + \nabla \cdot \alpha_k \boldsymbol{\tau}_k + \alpha_k \rho_k \mathbf{g} + \mathbf{M}_k \tag{2}$$

Above k=1,2 is the index of either phase, α_k is the phase volume fraction, ρ_k is the phase density, τ_k is the phase shear stress tensor, $\mathbf{u}_k$ is the phase velocity vector, p is the static pressure field, and $\mathbf{g}$ is the gravitational acceleration vector. $\mathbf{M}_k$ is the momentum exchange term between the phases which consists of the drag force, found by scale analysis to be the dominant force for drifting snow [13]. The snow phase shear stress term in the momentum equation above requires a snow viscosity parameter. Many snow compactive viscosity models are available for very low rates of strain typical of settling snow, the latest by Teufelsbauer [16] including a review of the main models in the literature. However, nothing was available at the high rates of strain of the simulation above. It proved practical to use a dynamic viscosity equivalent to that of air since the snow concentrations were extremely low and the flow dilute and practically one-way coupled. Even so solving the snow phase momentum equation separately still allowed accounting high drift where it occurred close to the cube and led to a much more accurate drift shape.

The objective of this paper is to present a viable snow phase viscosity model at high rates of strain and two-way coupled situations such as snow creep and saltation, for the simulation of drifting snow using an Eulerian-Eulerian system of equations for interpenetrating phases. Section 2 discusses the high rate of strain viscosity model and initial validation results are presented in Section 3.

2 HIGH RATE OF STRAIN SNOW VISCOSITY MODEL

The snow phase viscosity is derived by matching the total momentum of a number of ideal spherical drifting particles within a control volume, with the total momentum of the same control volume containing an equal amount of the equivalent viscous fluid to the particles. Drifting snow particles move in transient hops and bounce over the snowbed surface but since drifting snow is easily observed in sustained steady-state mode in natural and controlled environments the motion of the spherical particles can be considered steady-state *in the average sense*. This approximation is only used for the purpose of deriving an expression of the snow phase Newtonian viscosity model. An analytical analysis showed that at steady-state the difference between the velocity of a rolling sphere and the average velocity of the driving airflow is small enough that a Stokes drag expression can be accurately used to represent the drag force. Furthermore a scale analysis showed that the rolling friction force is negligible compared to the drag force so the rolling friction force was not retained in the snow viscosity analysis. Besides, the effects of surface friction forces between the rolling particle and snowbed asperities is already implicitly included in the surface threshold shear stress $\tau_t = \alpha_a \rho_a u_t^2$ where α_a is the air volume fraction, ρ_a the air density and u_t the threshold friction velocity.

The derivation of the drifting snow phase dynamic viscosity starts with the momentum balance equations of the air and snow phase respectively for fully-developed steady-state flow in a control volume containing a number of rolling particles on the snowbed and having the same height as a particle,

$$-\alpha_a \frac{dP}{dx} - F_{d,v} = 0$$

$$-\alpha_s \frac{dP}{dx} + F_{d,v} + \alpha_s \nu_s \frac{d^2 u_s}{dy^2} = 0$$

Above dP/dx is the pressure gradient, $F_{d,v}$ is the drag force per unit volume, α_s the snow phase volume fraction, ν_s the snow phase kinematic viscosity and u_s its velocity. The air flow shear stress term does not appear in the airflow momentum equation since at the particle diameter height over the snowbed the airflow is in the laminar sublayer and close to being linear. Eliminating the drag force and integrating for the snow phase velocity we get,

$$u_s(y) = \frac{1}{2\alpha_s \nu_s} \frac{dP}{dx} y^2 + \frac{\alpha_a \rho_a u_t^2}{\alpha_s \nu_s \rho_s} y$$

ICWE14 June 21-26, 2015 | Porto Alegre - Brazil 14th INTERNATIONAL CONFERENCE ON WIND ENGINEERING

ρ_s is the snow phase density which appears as a result of enforcing a Newtonian shear stress boundary condition at the snowbed surface. The final step consists of matching the total momentum of the snow particles in the control volume with the same amount of Eulerian viscous snow fluid. This results in the following expression for the drifting snow kinematic viscosity,

$$\nu_s = \frac{\frac{dP}{dx} d_p}{6\varepsilon_s} + \frac{\tau_t}{2\rho_s \varepsilon_s}$$

Above, $\varepsilon_s = \alpha_s V_p / d_p$ is the snow phase rate of strain, where d_p is the snow particle diameter and V_p is the snow particle velocity. The above viscosity expression basically means that the kinematic viscosity of the drifting snow phase has a pressure component deriving from the pressure change across a particle and a shear stress contribution deriving from the threshold shear stress required to make the snow phase drift. Alternatively one can eliminate the pressure gradient in the air and snow phase momentum equations and retain the volumetric drag force, redefining the kinematic viscosity as,

$$\nu_s = -\frac{F_{d,v} d_p}{6\alpha_a \varepsilon_s} + \frac{\tau_t}{2\rho_s \varepsilon_s}$$

The two expressions of the snow phase kinematic viscosity are equivalent but the one using the volumetric drag force explicitly highlights the concurrency between the two terms. The kinematic viscosity is basically a combination of the snowbed resistance expressed as threshold shear stress which tends to increase the viscosity, and the aerodynamic drag force on the particle which tends to induce motion and reduce the viscosity. The drag force drifting snow viscosity expression was implemented in the OpenFOAM® solver along with other modifications, and the resulting solver is now dubbed driftingSnowFoam.

3 VALIDATION WITH WIND TUNNEL DATA

3.1 Experimental setup

An initial validation of the drifting snow viscosity model presented in the previous section was done using data from a controlled drifting snow experiment carried out by the Tohoku university group [17] at the Cryospheric Environment Simulator (CES) of the Shinjo Branch of the Snow and Ice Research Center (SIRC) at the National Research Institute for Earth Science and Disaster Prevention (NIED) in Japan. In the Tohoku experiments, the profiles of mass flux of drifting snow, wind velocity, and turbulence statistics were measured under several different wind speed conditions and at different locations in the wind tunnel working section shown in Figure 2. Loose snow is deposited in a 2 cm deep gutter along the length of the tunnel floor which is preceded by a 1 m fetch of frozen non-drifting hard snow in order to generate a non-equilibrium saltation layer. The measured airflow velocity and turbulence kinetic energy at station X=0m were used as boundary conditions for the numerical simulations. These profiles are shown in Figure 3 where Z_r=0.2 m and U_r≈7.0 m/s are the reference height and airflow velocity.

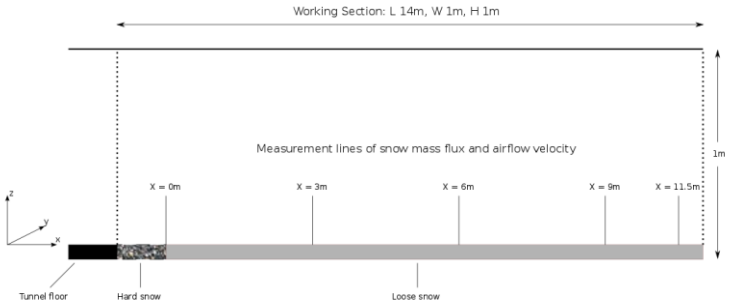

Figure 2. Side view of the mid-section of the wind tunnel setup (flow direction from left to right).

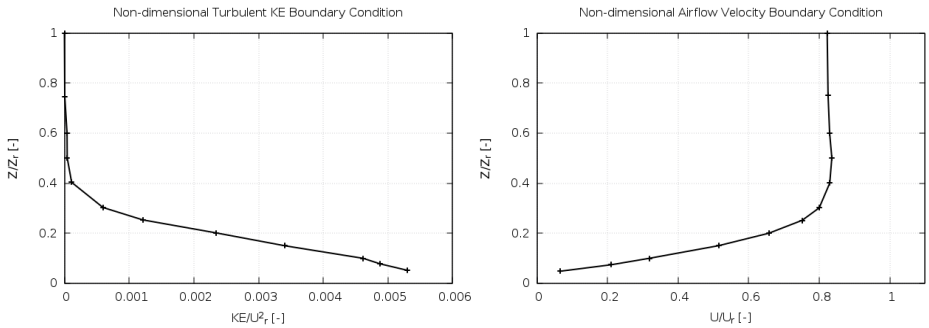

Figure 3. Numerical inlet boundary conditions, measured in the wind tunnel at X=0 m.

Samples of the snow particles used in the experiment are shown in Figure 4. The experiment snow particles are quite irregular and bulky exceeding 1 mm in length quite often but rarely smaller than 0.50 mm in either length or width, which implies a particle distribution with an average diameter larger than 0.50 mm. Particle sizes occurring in natural snow and mechanical breakage phenomena usually obey a two-parameter Gamma distribution be it as aggregate on the ground [18] or drifting above it [19]. This analysis focuses on the distributions shown in Figure 5 the use of which is discussed in the next section.

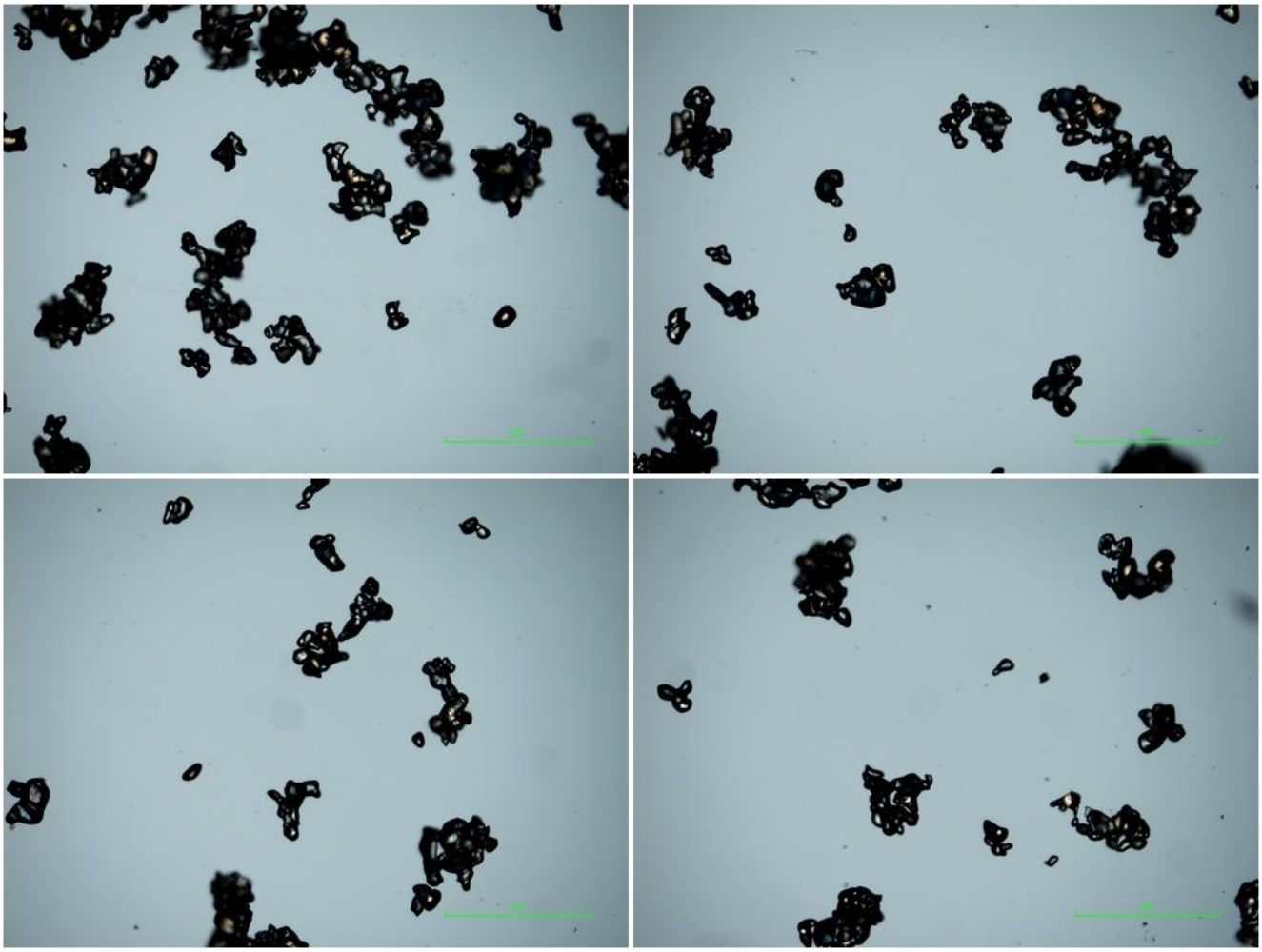

Figure 4. Samples of the experiment snow particles.

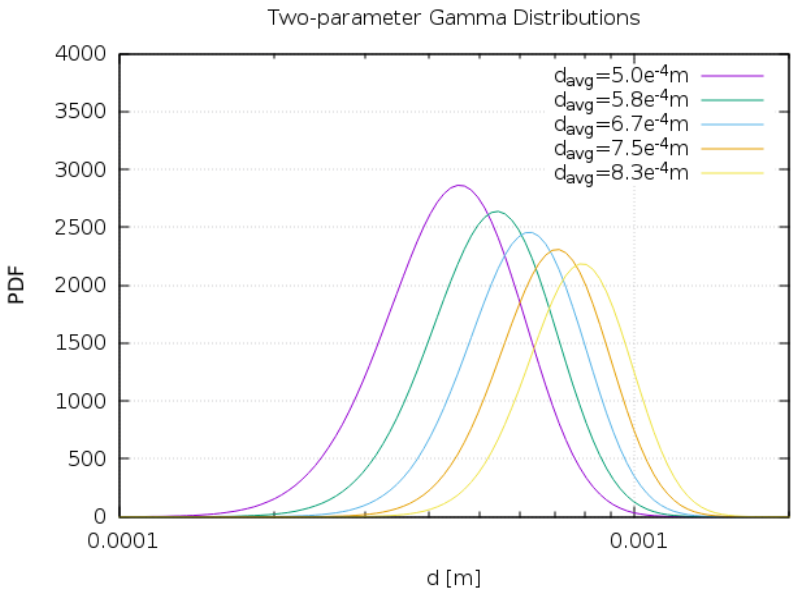

Figure 5. Two-parameter Gamma distributions evaluated in the numerical analysis.

3.2 Numerical setup

The 2D computational mesh used for the simulations is shown in Figure 6. Above is a close-up of the mesh at the inlet of the computational domain of the wind tunnel at X=0m, with the loose snow layer in the gutter shown in white. The mesh is fully structured hexahedral with a transverse element size of 4 mm in the gutter and at the top of the tunnel. The longitudinal element size in the flow direction along the X-axis is about 6 cm. Tests were carried out with a mesh twice finer in both directions and the results varied by less than 15% so results obtained from the present mesh can be reasonably considered mesh-independent. Simulations were carried out at a threshold shear stress of 0.052 Kg/(m.s^2) which is the minimum experimentally observed value for drifting.

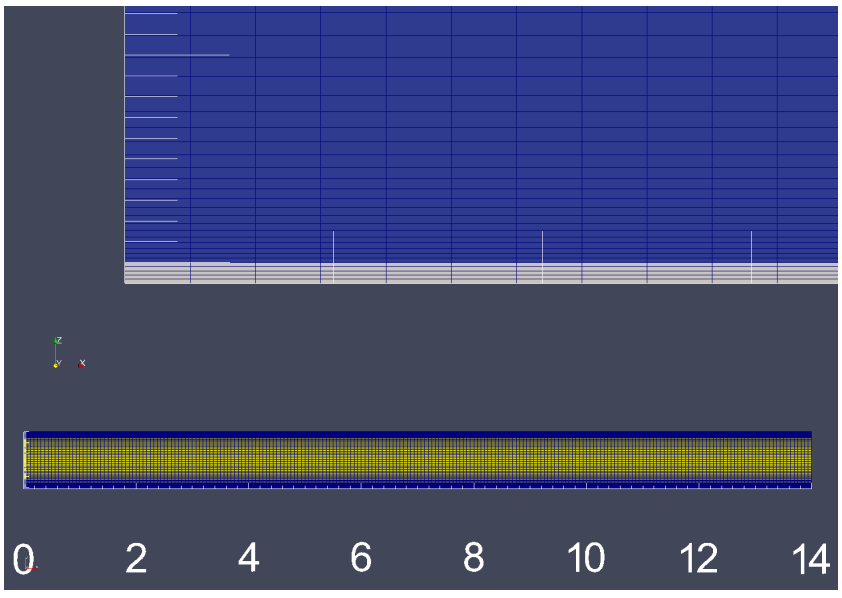

Figure 6. Close-up of the numerical mesh near the tunnel inlet showing the snowbed in the gutter (above), and overall view of the mesh (below).

3.3 Results and discussion

In this section the numerical results of snow flux, airflow velocity, turbulent kinetic energy and snow transport are compared to the experimental measurements. Initial comparisons were done based on single particle diameter results and it was quickly found that simulations with smaller particle diameters resulted in too much snow flux in the suspension layer and the upper half of the saltation layer due to excess erosion of the snowbed and flow separation. They also exhibited too little snow flux in the lower half of the saltation layer and could not provide a long enough measurement window of stable snowbed conditions as it occurred in the experiment. The experimental measurement window is a few of minutes of flow time with negligible erosion of the snowbed simultaneously at all measurement stations, of which 30 s were used to perform the measurements consecutively at all four stations. The simulations with the larger diameters on the other hand had too much snow flux in the lower saltation layer, too little in the suspension layer and the upper half of the saltation layer but exhibited the correct snowbed dynamics of the experimental measurements conditions. The intermediate diameter simulations had intermediate accuracy in the upper saltation layer and were quite inaccurate everywhere else. Finally all simulations of single particle sizes had the wrong shapes of snow flux curves and very poor agreement with the airflow measurements. It became clear that the experimental measurements were strongly influenced by the snowbed particle size distribution since snow flux in the suspension layer and the upper half of the saltation layer depended on the smaller and intermediate size particles, while snow flux in the lower half of the saltation layer depended on large size particles the inertia of which provided snowbed stability. The focus naturally shifted to analyzing numerical results obtained by combining the results of the single diameter simulations according the probability distribution weights of the single diameter classes in the probability distributions shown in Figure 5. The simulations were performed for seven particle diameters, namely 0.1, 0.3, 0.5, 0.7, 0.9, 1.1, and 1.3 mm. The individual particle diameter simulations were then combined according to the statistical weights of the particle classes of the Gamma distributions in Figure 5 to provide distribution solutions with average particle diameters of 0.50, 0.58, 0.67, 0.75 and 0.83 mm. Several average particle diameters were evaluated since the average particle diameter in the experiment was not measured.

3.3.1 The snow flux comparisons

The transient change in snow flux at the four measurement stations in the tunnel is shown in Figure 7 for the experimental measurements and three numerical average particle distribution diameters: 0.50, 0.67 and 0.83 mm. At the first measurement station at X=3.0 m (first row) which is closest to the upstream hard snow fetch, the best agreement in the saltation layer below Z=0.04 m is found at the smallest numerical average particle diameter of 0.50 mm (first column). However as we move downstream to the measurement stations at X=6.0, 9.0 and 11.5 m (second, third and fourth rows respectively) the best agreement is found at the numerical average particle diameter of 0.67 mm (second column). The largest numerical average particle diameter of 0.83 mm (third column) always provides the worst agreement with experiment implying a distribution with such an average particle diameter is much too heavy to be transported by the airflow and provide the observed snow fluxes in the saltation layer. The shape of the snow flux curve can also be indicative of the type of saltation and relative average size of snow particles. The experimental snow flux curve at X=3.0 m has a somewhat larger slope than the other three locations and is more convex. This indicates there is more flux at the higher levels in the suspension layer and the upper saltation layer, typically by smaller particles bouncing relatively high through the saltation layer and lifted by turbulence into the suspension layer. On the other hand the shapes of the experimental snow flux curves at X=6.0 m and 9.0 m downstream are much flatter with smaller slopes suggesting more flux in the lower levels of the saltation layer which is due to the larger particles, hence the larger average distribution diameter. The experimental snow flux curve at X=9.0 m has a distinct sudden increase between Z=5 cm and Z=6 cm, right at the upper limit of the saltation layer where increases in the experimental turbulence kinetic energy due to high airflow shear are reported. Turbulence is normally responsible for transport of particles to and in the suspension layer so the turbulent shear layer in that region is probably behind the sudden increase in snow flux. The downstream increase in average distribution diameter necessary to match the experimental result highlights as well the role of particle collisions in sustaining drifting snow in a developing saltation layer. As the drifting layer develops and aerodynamic entrainment is hindered ongoing collisions dislodge particles on the snowbed surface making it easier to lift larger and larger particles in the saltation layer, with the smaller particles lifted by turbulence into the suspension layer. Both snow flux curves at X=9.0 m and 11.5 m show a convex shape reminiscent of the snow flux curve at X=3.0 m in the upper half of the saltation layer between Z=2cm and 4 cm. This increased snow flux at the upper levels is again indicative of particle rebound due to collisions on the snowbed but here it comes at the heels of the increased flux of particles above the saltation layer at X=9.0 m which seems to have led to a cascade of particles collisions between X=9.0 m and 11.5 m.

The process eventually reaches equilibrium as reported by the experiment authors so there seems to be enough supply of upstream particles to sustain drifting through collisions which makes up for the loss of airflow momentum in the saltation layer through two-way coupling with the particle phase. With larger particles drifting into the saltation layer due to collisions it is logical to see a downstream increase in the average distribution diameter required to match the numerical solutions with the experimental results.

The general trend in the comparisons is that the smallest average diameter numerical snow flux is closest to experimental snow flux at the highest level of the saltation layer while the reverse is true for the larger average particle diameter. This again is due to the fact that the lower levels of the saltation layer are generally populated with the larger heavier particles which do not bounce as high as the smaller lighter particles and tend to move mostly in small hops and rolls, while the smaller lighter particles bounce high and are lifted by turbulence. This inertial segregation which was pointed out as early as the first studies on aeolian particle transport [1] is correctly reproduced by the present novel numerical formulation. However it was necessary to compute several different solutions each with a different particle diameter to be able to point it out since the present formulation can only account for one particle diameter at a time. Schmidt [19] points out that particle size distributions change with height over the snowbed and, as already discussed, it is reasonable to expect they will also change in the downstream direction in a developing boundary layer with a changing surface shear stress. It is possible to account for an entire distribution of particle diameters by solving a transport equation for the probability density function of the distribution. This would also allow taking in consideration collisions of particles of different sizes with each other in the lower half of the saltation layer and on the snowbed. This is an improvement to the code that is planned for future versions and it should also allow accounting for the changes in the particle size distribution with height and downstream.

In the present numerical simulations the agreement with the experimental snow flux is quite poor above Z=0.04 m which is the onset of the suspension layer as found by the authors of the experiment. This region of the drifting layer is populated by the lighter particles which reach it mainly through collisions and turbulent lift as discussed. Unfortunately there is no collision model implemented in the code yet so it is not possible to account for particle transport in the suspension layer by collisions off the snowbed. There remains the question of particle transport in the suspension layer by turbulence. The turbulence model implemented by the authors in driftingSnowFoam is the realizable K-epsilon applied to the airflow only without explicit two-way coupling of the turbulence to the particle phase. The two-way coupling between the particle phase and the airflow turbulence is a complex matter consisting of two concurrent processes. On one side there is damping/production of turbulence by the particle phase consisting of the addition of source and sink terms to the k-epsilon equations which is already used in the context of mixture models [4]. On the other side there is added momentum to the particle phase that can be important at the top of the saltation layer and which requires new turbulent terms to be added to the particle phase momentum equations. The Gosman turbulent model accounts for both these effects [23] but is not included in the present version of the solver. Initial tests with a simplified version of the added turbulent momentum to the particle phase equations produced some improvement to the snow flux in the suspension layer for small particles with a diameter of 0.2 mm. The improvement can be seen in the snow flux curves in Figure 8 and work on a full integration of the Gosman model in the dilute context of drifting snow in the saltation and suspension layers is already underway.

3.3.2 The airflow comparisons

The numerical results of airflow velocity at the measurement stations are shown in Figure 9 for the three particle size distributions examined and following the same format as in Figure 7. Except for the initial station at X=3.0 m and for the average distribution diameter of 0.50 mm (first row and column) there is substantial flow deceleration up to Z=0.1 m where most of the particles are drifting, a region including the full saltation layer and the initial part of the suspension layer. Flow deceleration occurs as a result of snowbed friction and particle blockage in the saltation layer, a two-way coupling phenomenon observed regularly in aeolian transport of particles [1]. As far as concerns the present simulations this flow deceleration is akin to a stagnation zone where k-epsilon turbulence models are known to overproduce turbulent kinetic energy [20].

A quantitative comparison to the experimental results can be done in Figure 10 where the experimental and numerical turbulent kinetic energy profiles are compared at measurement station X=11.5 m, the furthest downstream. The hard snow curve is one with the tunnel gutter completely filled with frozen non-drifting hard snow. The loose snow curve on the other hand is one where the snow is allowed to drift. As mentioned by the experiment authors there is overall turbulent energy production due to the particles and especially at the top of the saltation layer at Z=0.04 m where the airflow accelerates. This turbulent energy production is evident at Z=0.04 m in the numerical curves but there is clearly too much of it due to the shortcomings of the k-epsilon model. Since the particle effect on

turbulent kinetic energy and dissipation rate is not taken into account in the present formulation the turbulent kinetic energy overproduction is happening at the expense of excessive airflow deficits as seen in the numerical comparison to experiment. However care should be exercised in comparing to the experimental measurements of turbulent kinetic energy since the experiment authors report that the ultra-sonic anemometer used in the experiment cannot measure small scale fluctuations of frequencies higher than 20 Hz. Therefore turbulence kinetic energy in the high frequency range is not included in the measurements. Fortunately this error is expected to be most important very close to the snowbed 5 cm below the lowest measurement point in the region of the smallest eddies, which are expected to have a length scale comparable to the size of the bed asperities themselves comparable to the particle sizes.

The non-dimensional turbulent kinetic energy profiles at all measurement stations are shown in Figure 11 for the three average distribution diameters 0.50, 0.67 and 0.83 mm. The turbulent kinetic energy is non-dimensionalized by the square of the reference velocity at the reference height Z_r=0.2 m. In Figure 9 the best agreement between numerical and experimental results is always at X=3.0 m for all average diameters. This again is a direct result of the turbulent energy production which is smallest at X=3.0 m as can be seen in Figure 11. In particular the turbulent kinetic energy for d_{avg}=0.50 mm at X=3.0 m (top left plot in Figure 9) is the smallest of all which is the reason for the best agreement seen in Figure 9.

Fixes to the turbulent kinetic energy overproduction are available in the literature in the form of a bound on the turbulence time scale [21] or a linearized production term [22] and will be investigated.

3.3.3 The snow transport comparisons

The last analysis is a comparison between the experimental and numerical transport rates of snow. The snow transport rate is obtained by integrating the snow flux from the top of the snowbed at Z=0 m up to the top of the saltation layer at Z=0.05 m per the experimental procedure and represents the snow transport by saltation. The results are plotted in Figure 12 for all three average distribution diameters at the four measurement stations. The distribution with d_{avg}=0.50 mm is the most accurate at X=3.0 m while the distribution with d_{avg}=0.67 mm is the most accurate at the other three stations further downstream. The distribution with the largest average diameter d_{avg}=0.83 mm is the least accurate everywhere. These results follow naturally from the snow flux results discussed above. They also underline the ability of the two-way coupled approach to accurately model drifting snow in the saltation layer. The experimental trend is reproduced numerically except at the last measurement station X=11.5 m where the drifting layer is reported to have reached equilibrium in the experiment. Fully-developed drifting layers normally require snowbed surface particle collisions to counterbalance the drop in fluid shear stress due to flow deceleration. In the present case collision forces are not included yet in the formulation so the drifting layer cannot develop fully. On the other hand judging from Figure 11 the increase in numerical turbulent kinetic energy is largest at X=11.5 m meaning the numerical airflow is slowest there so it is no surprise snow transport decreases. This finding stresses again the need for including collision forces in the formulation and a Hertzian contact model is presently under development to be included and tested in the next version of the solver.

4 CONCLUSIONS AND FUTURE WORK

A novel drifting snow viscosity model was presented along with initial validation results against a controlled wind tunnel drifting snow experiment. This novel viscosity model allowed the Eulerian-Eulerian simulation of drifting snow in the saltation layer without resorting to empirical correlations such as used by other Eulerian methods. It was also found necessary to take into consideration the size distribution of the particles to have agreement with the experimental data. This is due to the inertial segregation that happens in aeolian transport of particles over hard surfaces. The inertial segregation manifested itself going from the saltation layer up to the suspension layer and also downstream as a result of the drifting layer shifting from non-equilibrium to equilibrium. Agreement with the experimental data was very bad in the suspension layer since the present two-way coupled formulation does not include collision forces on particles impacting the snowbed and the turbulent lift responsible for transporting smaller particles into the suspension layer. Agreement with the experimental data of airflow velocity was bad in general and found to be cause by the k-epsilon model's overproduction of turbulent kinetic energy in the saltation layer and lower suspension layer whch are effectively stagnation zones due to the presence of the drifting particles.

It remains that the present two-way coupled formulation is successful at predicting particle flux in the saltation layer in both equilibrium and non-equilibrium situations. Since particle freezing and thawing is not considered the model can easily be extended to aeolian transport of sand and even riverbed sediment transport, to give only a couple of examples.

Given the stated limitations of this approach it is necessary to make the following implementations:

- A Probability Density Function (PDF) transport equation is necessary to be able to reproduce the effects of an entire particle size distribution without having to compute several single size simulations. A PDF transport equation will also allow accounting for inter-particle collisions in and over the snowbed in the lower saltation layer.
- A collision force model and turbulent lift term are necessary in order to generate transport of particles in the suspension layer and be able to simulate equilibrium drifting layers. A simplified turbulent lift model has already been tested with some success and a Hertzian collision model has been developed and is being implemented.
- A correction for the overproduction of turbulent kinetic energy in the drifting layer by the k-epsilon model is necessary since it will not be possible to obtain correct airflow profiles without it. It is also necessary to implement damping/production of turbulent kinetic energy by particles.

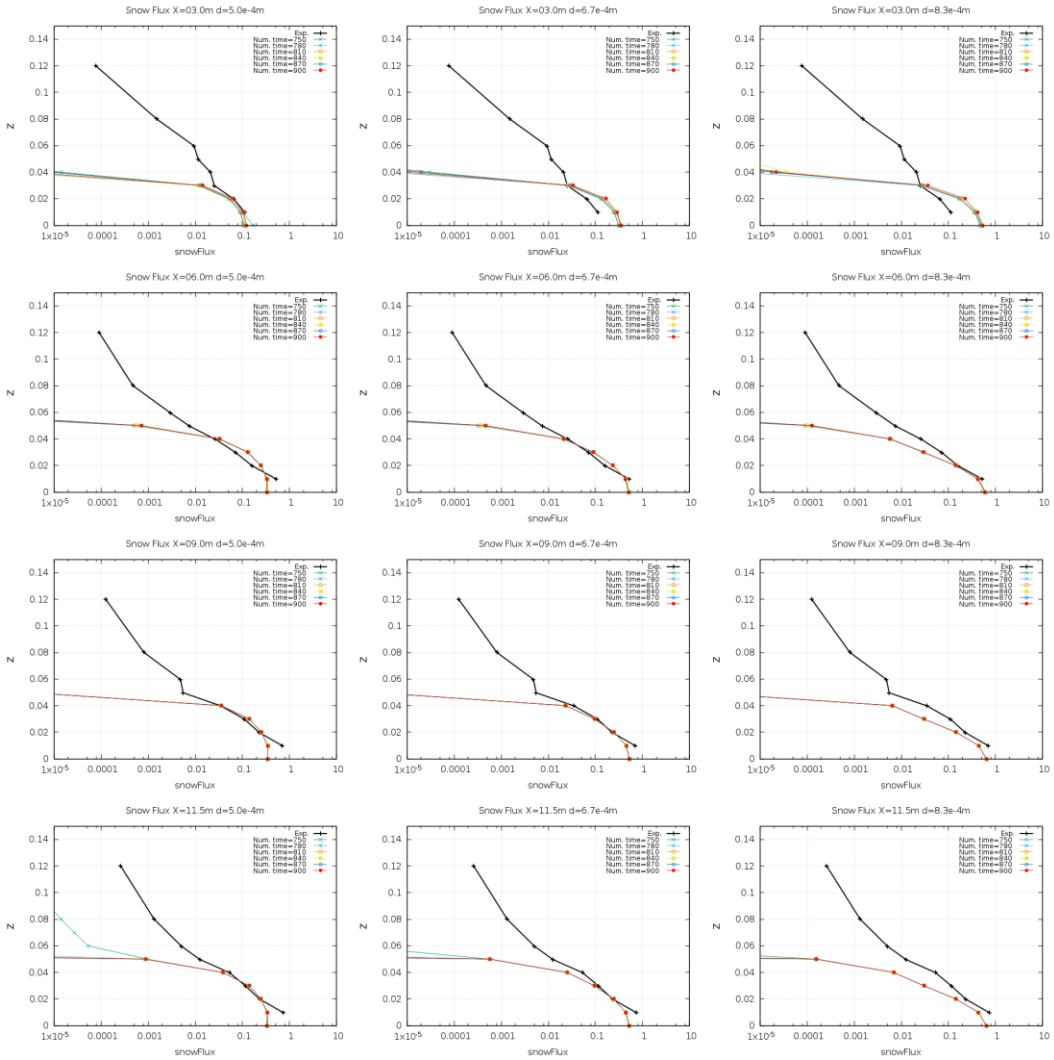

Figure 7. Comparisons of numerical to experimental snow flux at the four measurement stations (top to bottom) for increasing average particle distribution diameter (left to right).

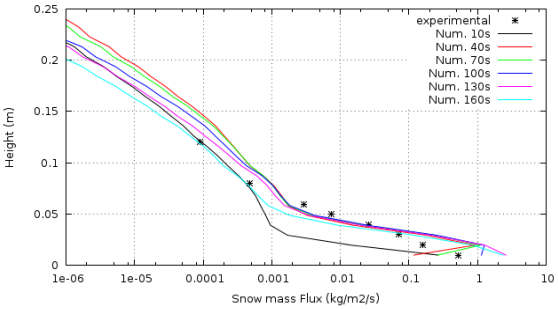

Figure 8. Snow flux in the suspension layer at X=6.0 m with a simple particle turbulent momentum model.

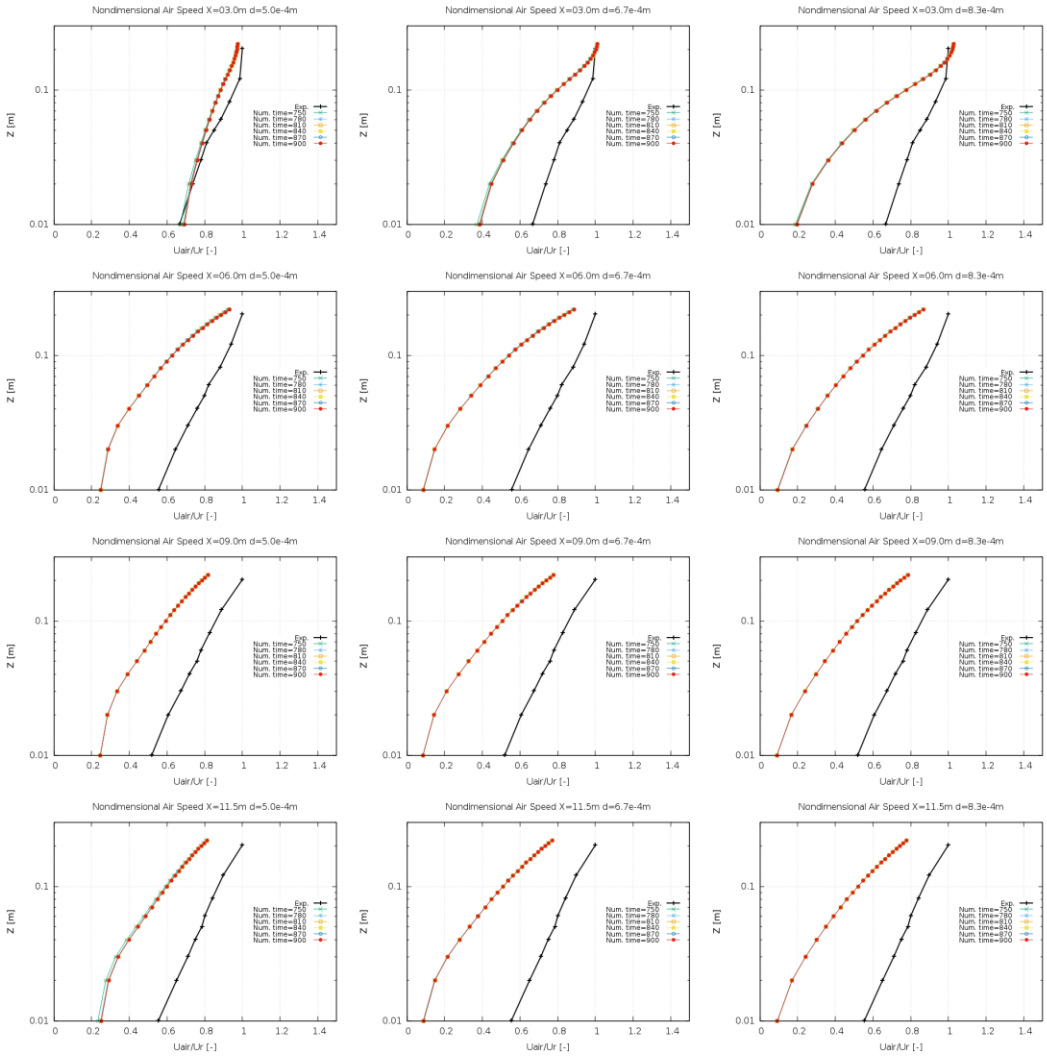

Figure 9. Comparisons of numerical to experimental non-dimensional airflow at the four measurement stations (top to bottom) for increasing average particle distribution diameter (left to right).

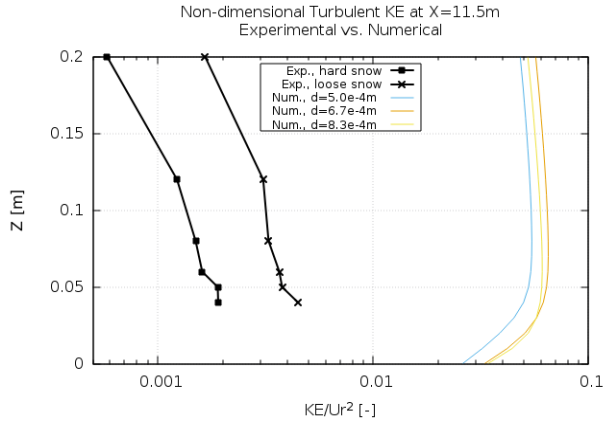

Figure 10. Comparison of experimental and numerical turbulent kinetic energy at X=11.5 m.

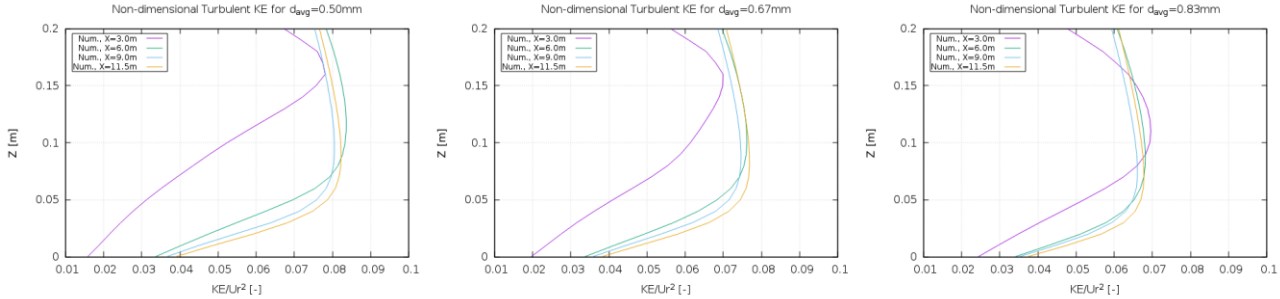

Figure 11. Turbulent kinetic energy variation by distribution diameter at all measurement stations.

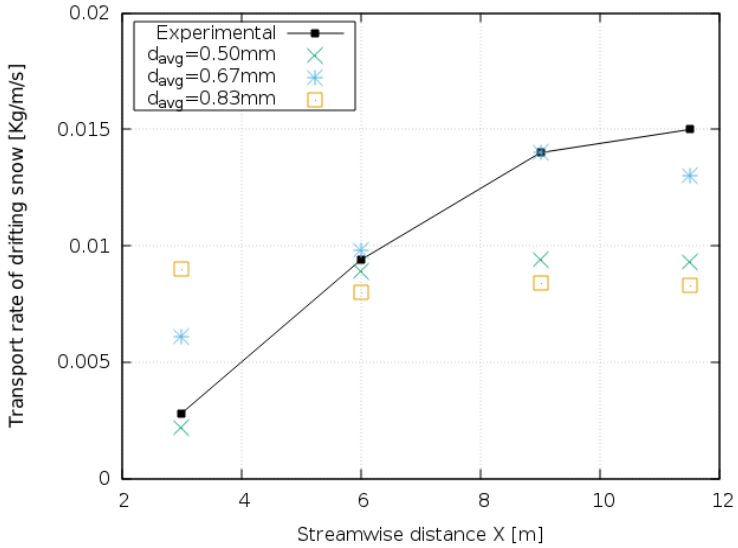

Figure 12. Comparison of experimental and numerical snow transport from 0 to 5 cm height.

ACKNOWLEDGMENTS

The authors extend their warmest thanks to Dr. Tsubasa Okaze for sharing his experimental data and his continued support, as well as Dr. Akashi Moshida and Dr. Yoshihide Tominaga.

The simulations presented in this paper as well as simulations towards ongoing improvements to the formulation are done on the Arctur Universe cloud computing platform (www.arctur.si).

REFERENCES

[1] R. Bagnold. The physics of blown sand and desert dunes. London, Methuen, 1941.

[2] B.E. Lee, J.Y. Tu, and C.A.J. Fletcher. On numerical modeling of particle-wall impaction in relation to erosion prediction: Eulerian versus Lagrangian method. *Wear*, 252:179–188, 2002.

[3] T. Uematsu, T. Nakata, K. Takeuchi, Y. Arisawa, and Y. Kaneda. Three-dimensional numerical simulation of snowdrift. *Cold Regions Science and Technology*, 20:65–73, 1991.

[4] M. Naaim, F. Naaim-Bouvet, and H. Martinez. Numerical simulation of drifting snow: erosion and deposition model. Annals of Glaciology, 26: 191–196, 1998.

[5] Y. Tominaga and A. Mochida. CFD prediction of flowfield and snowdrift around a building complex in a snowy region. *Journal of Wind Engineering and Industrial Aerodynamics*, 81:273–282, 1999.

[6] J.W. Pomeroy and D.M. Gray. Saltation of snow. *Water Resources Research*, 26(7):1583–1594, 1990.

[7] T. Okaze, A. Mochida, Y. Tominaga, M. Nemoto, Y. Ito, and T. Shida. Modeling of drifting snow development in a boundary layer and its effect on windfield. In *The Sixth Snow Engineering Conference*, Whistler, B.C., Canada, June 1-5 2008.

[8] Y. Tominaga, T. Okaze, and A. Mochida. CFD modeling of snowdrift around a building: overview of models and evaluation of a new approach. *Building and Environment*, 46:899–910, 2011.

[9] B. Bang, A. Nielsen, P.A. Sundsbø, and T. Wiik. Computer simulation of wind speed, wind pressure and snow accumulation around buildings (SNOW-SIM). *Energy and Buildings*, 21(3):235–243, 1994.

[10] J.H.M. Beyers. Numerical modeling of the snowdrift characteristics surrounding the SANAE IV research station. Ph.d. dissertation, Department of Mechanical Engineering, University of Stellenbosch, 2004.

[11] J.H.M. Beyers and B. Waechter. Modeling transient snowdrift development around complex three-dimensional structures. Journal of Wind Engineering and Industrial Aerodynamics, 96:1603–1615, 2008.

[12] P.A. Sundsbø. Numerical simulations of wind deflection fins to control snow accumulation in building steps. Journal of Wind Engineering and Industrial Aerodynamics, 74-76:543–552, 1998.

[13] Gauer, P. 1999. Blowing and drifting snow in Alpine terrain: a physically-based numerical model and related field measurements. *Eidg. Inst. Schnee- und Lawinenforsch.* Mitt. 58.

[14] Z. Boutanios and H. Hangan. Eulerian-Eulerian CFD snowdrift analysis. In *The 13th International Conference of Wind Engineering*, Amsterdam, the Netherlands, July 10-15, 2011.

[15] T.K. Thiis. A comparison of numerical simulations and full-scale measurements of snowdrifts around buildings. Wind and Structures, 3(2):73–81, 2000.

[16] H. Teufelsbauer. A two-dimensional snow creep model for alpine terrain. Natural Hazards, 56:481-497, 2011.

[17] T. Okaze, A. Mochida, Y. Tominaga, M. Nemoto, T. Sato, Y.Sasaki, and K. Ichinohe. Wind tunnel investigation of drifting snow development in a boundary layer. *J. Wind Eng. Ind. Aerodyn.*, 104-106:532–539, 2012.

[18] W.F. Budd. The drifting of nonuniform snow particles. *Stud. Antarctic Meteorol., Am. Geophys. Union, Antarctic Res. Ser.*, 9:59-70, 1966.

[19] R.A. Schmidt. Vertical profiles of wind speed, snow concentration, and humidity in blowing snow. *Boundary Layer Meteorology*, 23:223-246, 1982.

[20] W.C. Strahle. Stagnation point flows with freestream turbulence – The matching condition. *AIAA J.*, 23:1822-1824, 1985.

[21] P.A. Durbin. On the k-3 stagnation point anomaly. *Int. J. Heat and Fluid Flow*, 17:89-90, 1996.

[22] V. Guimet and D. Laurence. A linearised turbulent production in the k-epsilon model for engineering applications. In *Engineering Turbulence Modelling and Experiments 5*, 157-166, 2002.

[23] A.D. Gosman, C. Lekakou, S. Politis, R.J. Issa and M.K. Looney. Multidimensional modeling of turbulent two-phase flows in stirred vessels. *AIChE Journal*, vol. 38(12):1946-1956.